

Projections of ITER Performance Based on Different Pedestal Temperature Scalings

K. Tharasrisuthi and T. Onjun

Sirindhorn International Institute of Technology,
Thammasat University, Pathum Thani, 12121, Thailand

O. Onjun

Department of Science Service, Ministry of Science
and Technology, Bangkok, 10400, Thailand

Abstract

Self-consistent modeling of the International Thermonuclear Experimental Reactor (ITER) has been carried out using the 1.5D BALDUR integrated predictive modeling code. In these simulations, the plasma parameters at the top of the pedestal are used as boundary conditions. These pedestal temperature models are based on three different pedestal width scalings: magnetic and flow shear stabilization width scaling [$\Delta \propto \rho s^2$], flow shear stabilization width scaling [$\Delta \propto (\rho R q)^{1/2}$], and normalized poloidal pressure width scaling [$\Delta \propto R(\beta_{0,ped})^{1/2}$]. These pedestal width scalings are combined with a pedestal pressure gradient model based on 1st ballooning mode stability limit to predict the pedestal temperature. These pedestal temperature models are used together with a core transport model, which is a combination of an anomalous transport and a neoclassical transport. An anomalous transport is calculated either using the Mixed Bohm/gyro-Bohm (Mixed B/gB) core transport model or the Multimode (MMM95) core transport model, while a neoclassical transport is computed using the NCLASS model. At the reference designed point (with 40 MW auxiliary heating: 33 MW NBI and 7 MW RF), it is found that the pedestal temperatures in all simulations are nearly the same. As a result, the performances with the same anomalous transport model are similar. However, the performance with MMM95 model is higher than that using Mixed B/gB model. It is also found that when MMM95 model is used, the ion temperature gradient (ITG) and trapped electron modes (TEM) are the most dominant modes. When Mixed B/gB model is used, the Bohm contribution is the most dominant term.

Keywords: Tokamak, H-mode, Pedestal, ITER

1. Introduction

The International Thermonuclear Experimental Reactor (ITER) is an international collaborative effort with an aim to demonstrate the scientific and technological feasibility of fusion energy using magnetic confinement fusion concept [1]. Due to the fact that high confinement mode (*H*-mode) discharges in tokamaks generally provide excellent energy confinement and have acceptable particle transport rates for impurity control, many fusion experiments such as ITER tokamak are designed to operate in the *H*-mode regime. The improved

performance of *H*-mode mainly results from the formation of the edge transport barrier, called the pedestal. Therefore, the performance of ITER depends sensitively on the pedestal width values.

In the previous ITER performance study by G. Bateman and his colleagues [2], the BALDUR integrated predictive modeling code with the Multimode (MMM95) anomalous transport model together with neoclassical transport, calculated using the Cheng-Hinton neoclassical model [3], was used to predict the plasma core profiles of ITER and, consequently, the performance of ITER. In that work, the

boundary conditions — which were taken to be at the top of the pedestal — were obtained from a predictive pedestal model based on magnetic and flow shear stabilization width model and first stability regime of infinite- n ballooning modes pressure gradient model [4]. It is also assumed that 40 MW of RF heating power is used as the auxiliary heating power, where 24 MW of RF heating power goes to thermal ions, and 16 MW of RF heating power goes to thermal electrons. Fast ions resulting from auxiliary heating are not considered. The heating produced by fusion reactions and the resulting fast alpha particles are added to the ohmic and auxiliary heating. The performance of ITER was evaluated in term of fusion Q . Note that fusion Q is the ratio of fusion power and applied heating power. An optimistic performance of ITER was obtained in that simulation with fusion Q of 10.6. In the later ITER performance study by T. Onjun and his colleagues [5], ITER simulations were carried out using the JETTO integrated predictive modeling code with the Mixed Bogm/gyro-Bohm (Mixed B/gB) anomalous transport model with NCLASS neoclassical transport [6]. In addition, the combination of 33 MW of Neutral Beam Injection (NBI) heating power and 7 MW RF heating power (similar to ITER reference design) was assumed. An optimistic performance of ITER with fusion Q of 16.6 was found. It was also found that the JETTO code predicts the strong edge pressure gradient, which would occur in the second stability regime of ballooning modes. In other words, the values at the top of the pedestal in the JETTO simulations are higher than those used in the BALDUR simulations.

In this work, the BALDUR integrated predictive modeling code is used to carry out simulations of the ITER plasma with the standard H -mode scenario. Two different anomalous core transport models, either MMM95 or Mixed B/gB models, are utilized for the core region. In addition, the neoclassical transport calculated using NCLASS module [6] is added to an anomalous transport. The effect of sawtooth oscillation is also included, where it is triggered by the Porcilli sawtooth model [7]. These BALDUR simulations are taking boundary conditions at the top of the pedestal. In this work, three pedestal temperature models are used to provide the boundary conditions. These

pedestal temperature models yield equally well, agreement with the pedestal data obtained from the ITPA pedestal database [8]. These pedestal temperature models are based on three different pedestal width scalings: magnetic and flow shear stabilization ($\Delta \propto \rho s^2$) [9], flow shear stabilization ($\Delta \propto (\rho R q)^{1/2}$) [4], and normalized poloidal pressure ($\Delta \propto R(\beta_{\theta, \text{ped}})^{1/2}$) [10], where ρ is the ion gyro radius, s is the magnetic shear, R is the major radius, q is the safety factor and $\beta_{\theta, \text{ped}}$ is the normalized pedestal pressure. The pedestal density is calculated using the same pedestal density model in Ref. [2]. This protocol will be used to investigate the performance of ITER.

This paper is organized as follows: brief descriptions for a BALDUR integrated predictive modeling code, anomalous transport models, and pedestal models are given in Sec.2. The ITER prediction using a BALDUR integrated predictive modeling code is described in Sec. 3, while conclusions are given in Sec. 4.

2. BALDUR Integrated Predictive Modeling Code

The BALDUR integrated predictive modeling code [11] is used to compute the time evolution of plasma profiles including electron and ion temperatures, deuterium and tritium densities, helium and impurity densities, magnetic q , neutrals, and fast ions. These time-evolving profiles are computed in the BALDUR integrated predictive modeling code by combining the effects of many physical processes self-consistently, including the effects of transport, plasma heating, particle influx, boundary conditions, the plasma equilibrium shape, and sawtooth oscillations. Fusion heating and helium accumulation are also computed self-consistently. The BALDUR simulations have been intensively compared against various plasma experiments, which yield an overall agreement with 10% relative RMS deviation [12, 13]. In BALDUR code, fusion heating power is determined by the nuclear reaction rates and a Fokker Planck package, to compute the slowing down spectrum of fast alpha particles on each flux surface in the plasma [11]. The fusion heating component of the BALDUR code also computes the rate of the production of thermal helium ions and the rate of the depletion of deuterium and tritium ions within the plasma core. In this work, two core transport models in

BALDUR will be used to carry out simulations of ITER. The brief details of these transport models are described below.

2.1 Mixed B/gB core transport model

The Mixed B/gB core transport model [14] is an empirical transport model. It was originally a local transport model with Bohm scaling. A transport model is said to be “local” when the transport fluxes (such as heat and particle fluxes) depend entirely on local plasma properties (such as temperatures, densities, and their gradients). A transport model is said to have “Bohm” scaling when the transport diffusivities are proportional to the gyro-radius times thermal velocity over a plasma linear dimension such as major radius. Transport diffusivities in models with Bohm scaling are also functions of the profile shapes (characterized by normalized gradients) and other plasma parameters such as magnetic q , which are all assumed to be held fixed in systematic scans in which only the gyro-radius is changed relative to plasma dimensions. The original JET model was subsequently extended to describe ion transport, and a gyro-Bohm term was added in order for simulations to be able to match data from smaller tokamaks as well as data from larger machines. A transport model is said to have “gyro-Bohm” scaling when the transport diffusivities are proportional to the square of the gyroradius times thermal velocity over the square of the plasma linear dimension. The Bohm contribution to the JET model usually dominates over most of the plasma. The gyro-Bohm contribution usually makes its largest contribution in the deep core of the plasma and plays a significant role only in smaller tokamaks with relatively low power and low magnetic field.

2.2 Multimode core transport model

The MMM95 model [15] is a linear combination of theory-based transport models which consists of the Weiland model for the ion temperature gradient (ITG) and trapped electron modes (TEM), the Guzdar-Drake model for drift-resistive ballooning modes, as well as a smaller contribution from kinetic ballooning modes. The Weiland model for drift modes such as ITG and TEM modes usually provides the

largest contribution to the MMM95 transport model in most of the plasma core. The Weiland model is derived by linearizing the fluid equations, with magnetic drifts for each plasma species. Eigenvalues and eigenvectors computed from these fluid equations are then used to compute a quasilinear approximation for the thermal and particle transport fluxes. The Weiland model includes many different physical phenomena such as effects of trapped electrons, $T_i \neq T_e$, impurities, fast ions, and finite β . Note that β is a ratio between plasma energy and magnetic energy. The resistive ballooning model in MMM95 transport model is based on the 1993 **ExB** drift-resistive ballooning mode model by Guzdar-Drake, in which the transport is proportional to the pressure gradient and collisionality. The contribution from the resistive ballooning model usually dominates the transport near the plasma edge. Finally, the kinetic ballooning model is a semi-empirical model, which usually provides a small contribution to the total diffusivity throughout the plasma, except near the magnetic axis. This model is an approximation to the first ballooning mode stability limit. Since the models were originally derived for circular plasmas, all the anomalous transport contributions to the MMM95 transport model are multiplied by κ^{-4} , where κ is the elongation.

2.3 Pedestal models

In the development of the pedestal temperature models described in Ref. [4], two ingredients are required: the pedestal width (Δ) and the pressure gradient ($\partial p / \partial r$). If the pedestal density, n_{ped} , is known, the temperature at the top of the pedestal (T_{ped}) can be estimated as:

$$T_{ped} = \frac{1}{2n_{ped}k} \left| \frac{\partial p}{\partial r} \Delta \right| \quad (1)$$

where k is the Boltzmann constant. In this work, three pedestal temperature models in Ref. [4] are selected. These pedestal temperature models yield equally well agreement with the pedestal data from the ITPA Pedestal Database [8]. These pedestal temperature are based on either the magnetic and flow shear stabilization width model ($\Delta \propto \rho s^2$) [9], the flow shear

stabilization width model ($\Delta\alpha(\rho Rq)^{1/2}$) [4], or the normalized poloidal pressure width model ($\Delta\alpha R(\beta_{\text{p,ped}})^{1/2}$) [10]. The detailed development of these pedestal temperature model can be obtained from Ref. [4].

The pedestal density, n_{ped} , is described by a simple pedestal density model. Since the pedestal density is usually a large fraction of line average density, n_l , the pedestal density is estimated as:

$$n_{\text{ped}} = 0.71n_l \quad (2)$$

This pedestal density model agrees with the pedestal data obtained from the ITPA pedestal database with 12% RMSE.

3. Results and Discussions

The BALDUR integrated predictive transport modeling code is used to carry out the simulations of ITER with the designed parameters ($R = 6.2$ m, $a = 2.0$ m, $I_p = 15$ MA, $B_T = 5.3$ T, $\kappa_{95} = 1.85$, $\delta_{95} = 0.33$ and $n_l = 1.0 \times 10^{20}$ m⁻³). In this work, an anomalous transport is calculated either using the Mixed B/gB transport model or using the MMM95 transport model, while the neoclassical transport is computed using the NCLASS module. The boundary conditions are provided at the top of the pedestal by the pedestal model described above. It is assumed that the electron and ion pedestal temperatures are the same values. In most simulations, the auxiliary heating power of 40 MW, which is a combination of 33 MW NBI heating power with 7 MW of RF heating power, is used. Figures 1 and 2 show the profiles for ion and electron temperatures and electron density as a function of major radius at a time of 300 sec using different models for predicting pedestal temperature. Note that these simulations are carried out using three different pedestal temperature models: the magnetic and flow shear stabilization width model (pedestal model 1), the flow shear stabilization width model (pedestal model 2), and the normalized poloidal pressure width model (pedestal model 3). The simulations using the Mixed B/gB core transport model and the MMM95 core transport models are shown in Fig. 1 and 2, respectively. It can be seen that the ion and electron temperature profiles for all simulations are peak profiles. For

the density profiles, the simulations with the Mixed B/gB transport model are peak profiles for all pedestal temperatures, while those in the simulations with the MMM95 transport model are quite unusual profiles. There are two small humps in the region about 60% of the plasma, which contain a smaller peak at the region close to the center of the plasma. However, this type of density profile is often observed in plasma simulations with the MMM transport model [12, 13]. It can also be seen that the pedestal temperatures and central temperatures in the simulation using the pedestal temperature based on normalized poloidal pressure width model is the highest, while those in the simulation using the pedestal temperature based on flow shear stabilization is the lowest. The results are summarized in Table 1. It is worth noting that the central temperatures obtained in the ITER simulation using the BALDUR code in Ref. [2] are higher than the results obtained in this work. This can be explained by the difference in the auxiliary heating used in each simulation. In the ITER simulations in Ref. [2], the auxiliary heating power was assumed to be 40 MW of RF heating power that is mainly applied in the plasma core region by employing a parabolic heating profile. This is an effective heating profile since most of the power is available at the center of the plasma. Consequently, a high central temperature can be obtained. The combination of NBI (33 MW) and RF (7 MW) heating power is used in this work. Because the ITER plasma density is considered to be a high density plasma, broader heating profiles are obtained, and consequently, lower temperature profiles, especially near the plasma center, are predicted.

The results of the ion pedestal temperature and the corresponding central ion temperature are summarized in Table 1. It can be seen that the pedestal temperature ranges from 2.4 keV to 2.8 keV, where the central temperature ranges from 10.3 keV to 16.5 keV. The values of ion pedestal temperature are not much different, but the central ion temperature is significantly different among the simulations using the Mixed B/gB core transport and the MMM95 core transport. The simulations using the pedestal model based on the normalized poloidal pressure width model yield the highest ion pedestal temperature and ion central temperature.

Figure 3 shows the ion thermal diffusivities as a function of minor radius from simulations using the Mixed B/gB transport model. It is worth noting that the ion temperature and density profiles for this simulation are shown in Fig. 1 and the pedestal model based on magnetic shear and flow shear stabilization width model is used for predicting boundary conditions. The "effective" thermal diffusivity, for example, is defined as the heat flux divided by the density times temperature gradient—with no separate contribution from convection. The total thermal diffusivities shown in Fig. 3 are the contributions from the Bohm and gyro-Bohm terms in the Mixed B/gB model as well as neoclassical transport, which has gyro-Bohm scaling. It can be seen in Fig. 3 that the Bohm contribution to the Mixed B/gB transport model is the dominant contribution to the ion thermal diffusivities everywhere in the plasma, except in the region close to the center of the plasma, where the neoclassical transport is the most dominant. It can be seen that the ion thermal diffusivity is less than $1 \text{ m}^2/\text{s}$ in the region from the center of the plasma to the radius of 80% of minor radius. This result for the transport is observed in all simulations with Mixed B/gB in this work. It is worth mentioning that the dominance of the Bohm contribution is similar to those results with the Mixed B/gB transport model reported in Refs. [12, 13].

Figure 4 shows the ion thermal diffusivities as a function of minor radius from a simulation using the MMM95 transport model for ITER. Note that the temperature and density profiles for this simulation are shown in Fig. 2, and that the pedestal model based on magnetic shear and flow shear stabilization width model is used for predicting boundary conditions. Note also that the Multi-mode ion thermal transport model consists of the ion temperature gradient and trapped electron modes, the drift-resistive ballooning modes, and the kinetic ballooning modes. It can be seen in Fig. 4 that the contribution from the ITG and TEM modes is the main contribution to most of the region of the plasma, except the region close to the center of the plasma, where the neoclassical transport is the most dominant. The thermal transport from the kinetic ballooning mode is significant in the region between normalized minor radius of 10% to 50%, whereas the resistive ballooning mode is small almost everywhere. It is worth

mentioning that in the region from the center of the plasma to the edge of plasma, the ion thermal diffusivity is less than $1 \text{ m}^2/\text{s}$, except at the last grid point, where the ion thermal is slightly above $1 \text{ m}^2/\text{s}$. Because of stronger thermal transport in the region near the edge of plasma when the Mixed B/gB transport model is used, a lower temperature profile is found. This result for the transport is observed in all simulations with MMM95 in this work.

In Fig. 5, the sawtooth mixing radius is plotted as a function of time. Note that the Porcilli model is used for calculating when the sawtooth crash occurs and the pedestal model based on magnetic shear and flow shear stabilization width model is used for predicting boundary conditions in this simulation. The details of the sawtooth trigger model and the sawtooth crash model can be found in Refs. [7, 16]. It is found in all simulations that almost all sawtooth crashes are triggered by trapped fast ions (Eq. 13 in reference [14]). Note that this condition is associated with fast ion stabilization. It can be seen in Fig. 5 that the sawtooth oscillations start at 82.4 sec and 140.9 sec for the simulations using Mixed B/gB and MMM95, respectively. The frequency of the sawtooth oscillation is almost the same for both transport model (0.8 Hz for Mixed B/gB and 0.7 Hz for MMM95 during the last 20 sec). The sawtooth mixing radius in the simulation using Mixed B/gB tends to be larger than that using MMM95 (116.1 cm for Mixed B/gB and 109.2 cm for MMM95 during the last 20 sec). It can be seen that the mixing radius of sawtooth oscillation in ITER is about half of the minor radius. This is an important issue for ITER. Further investigation is required.

In Fig. 6, the central ion temperature and alpha power is plotted as a function of time during time of 250 sec to 300 sec for the simulations using the Mixed B/gB and MMM95 models. Note that the pedestal model, based on magnetic shear and flow shear stabilization width model, is used for predicting boundary conditions in this simulation. It can be seen that the central ion temperature oscillates. This oscillation results from the sawtooth oscillation. The central ion temperature in the simulation using Mixed B/gB tends to be lower than that using MMM95 (9.1 keV for Mixed B/gB and 15.3 keV for MMM95 during the last 20 sec).

The fusion performance can be evaluated in term of Fusion Q , which can be calculated as

$$\text{Fusion } Q = \frac{5 \times P_{\alpha, \text{avg}}}{P_{\text{AUX}}} \quad (3)$$

where $P_{\alpha, \text{avg}}$ is an average alpha power and P_{AUX} is an auxiliary heating power (equal to 40 MW for these simulations). The results of average alpha power and fusion Q are summarized in Table 2. The higher alpha power production and fusion Q in the simulation using MMM95 results from higher temperature prediction. Note that the average alpha power is taken during the time of 250 sec to 300 sec.

4. Conclusions

Self-consistent simulations of ITER have been carried out using the 1.5D BALDUR integrated predictive modeling code. In these simulations, the boundary is taken to be at the top of the pedestal, where the pedestal values are described using the theoretical-based pedestal model. These pedestal temperature models are based on three different pedestal width scalings: magnetic and flow shear stabilization width scaling, flow shear stabilization width scaling, and normalized poloidal pressure width scaling. These pedestal width scalings are combined with a pedestal pressure gradient model based on ballooning mode limit to predict the pedestal temperature. The developed pedestal temperature models are used together with a core transport model, which is a combination of an anomalous transport and a neoclassical transport. The anomalous transport is calculated either using the Mixed Bohm/gyro-Bohm (Mixed B/gB) core transport model or Multimode (MMM95) core transport model, while the neoclassical transport is computed using the NCLASS model. At the reference designed point, it is found that the pedestal temperatures in all simulations are nearly the same. As a result, the performances with the same anomalous transport model are similar. However, the performance with MMM95 model is higher than that using Mixed B/gB model. It is also found that when the MMM95 model is used, the ion temperature gradient (ITG) and trapped electron modes (TEM) are the most dominant modes. When the Mixed B/gB model

is used, it appears that the Bohm contribution is the most dominant term.

5. Acknowledgements

T. Onjun is grateful to Prof. Arnold H. Kritz and Dr. Glenn Bateman for their generous support. This work is supported by National Research Council of Thailand, Thailand Toray Science Foundation, and Thammasat University Research Fund.

6. Referecnes

- [1] Aymar, R., Barabaschi, P. and Shimomura, Y. (for the ITER team), The ITER design, Plasma Phys. Control. Fusion, Vol. 44, pp. 519-566, 2002
- [2] Bateman, G., Onjun, T., and Kritz, A. H., Integrated Predictive Modelling Simulations of Burning Plasma Experiment Designs, Plasma Phys. Control. Fusion, Vol. 45, pp. 1939-1960, 2003
- [3] Chang, C. S. and Hilton, F. L., Effect of Impurity Particles on the Finite-Aspect-Ratio Ion Thermal Conductivity in a Tokamak Phys. Fluids, Vol. 29, pp. 3314-3316, 1986
- [4] Onjun, T., *et al.*, Models for the Pedestal Temperature at the Edge of H-mode Tokamak Plasmas, Physics of Plasmas, Vol. 9, pp. 5018-5030. 2002
- [5] Onjun, T., *et al.* Magnetohydrodynamic-calibrated Edge-localized Mode Model in Simulations of International Thermonuclear Experimental Reactor, Physics of Plasmas, Vol. 12, pp. 082513, 2005
- [6] Houlberg W. A., *et al.* Bootstrap Current and Neoclassical Transport in Tokamaks of Arbitrary Collisionality and Aspect Ratio, Physics of Plasmas, Vol. 4, pp. 3230-3242, 1997
- [7] Porcilli, F., Boucher, D., and Rosenbluth, M. N., Model for the Sawtooth Period and Amplitude, Plasma Physics and Controlled Fusion, Vol. 38, pp. 2163-2186, 1996
- [8] Hatae T., *et al.* Understanding of H-mode Pedestal Characteristics Using the Multimachine Pedestal Database, Nuclear Fusion, Vol. 41, pp. 285-294, 2001
- [9] Sugihara, M., *et al.*, A model for H-mode Pedestal Width Scaling Using the International Pedestal Database, Nuclear Fusion, Vol. 40, pp. 1743-1756, 2000
- [10] Osborne T. H., *et al.* H-mode Pedestal Characteristics in ITER Shape Discharges

- on DIII-D, Journal of Nuclear Materials, Vol. 266-269, pp. 131-137, 1999
- [11] Singer, C. E., *et al.* Baldur: A One-Dimensional Plasma Transport Code., Comput. Phys. Commun., Vol. 49, pp. 275-398, 1988
- [12] Hannum, D., *et al.*, Comparison of High-Mode Predictive Simulations Using Mixed Bohm/gyro-Bohm and Multi-Mode MMM95 Transport Models, Physics of Plasmas, Vol. 8, pp. 964-974, 2001
- [13] Onjun, T., *et al.*, Comparison of Low Confinement Mode Transport Simulations Using the Mixed Bohm/gyro-Bohm and the Multi-Mode-95 Transport Model, Physics of Plasmas, Vol. 8, pp. 975-985, 2001
- [14] Erba, M., *et al.* Development of a non-local Model for Tokamak Heat Transport in L-mode, H-mode and Transient Regimes. Plasma Phys. Control. Fusion, Vol. 39, pp. 261-276, 1997
- [15] Bateman, G., *et al.* Predicting Temperature and Density Profiles in Tokamaks, Physics of Plasmas, Vol. 5, pp. 1793-1799, 1998
- [16] Bateman, G., *et al.* Testing a Model for Triggering Sawtooth Oscillations in Tokamaks, Physics of Plasmas, Vol. 13, pp. 072505, 2006

Table 1: Summary of pedestal and central ion temperatures in the simulations for different pedestal width scalings using either Mixed Bohm/gyro-Bohm or Multi-mode transport model.

Pedestal Model	Pedestal Width	Mixed Bohm/gyro-Bohm model		Multi-mode model	
		$T_{i,ped}$ (keV)	$T_{i,0}$ (keV)	$T_{i,ped}$ (keV)	$T_{i,0}$ (keV)
1	$\Delta\alpha\rho s^2$	2.6	10.8	2.7	16.3
2	$\Delta\alpha(\rho Rq)^{1/2}$	2.4	10.3	2.4	16.1
3	$\Delta\alpha R(\beta_{0,ped})^{1/2}$	2.8	11.5	2.9	16.5

Table 2: Summary of alpha power production and fusion Q in the simulations for different pedestal width scalings using either Mixed Bohm/gyro-Bohm or Multi-mode transport model.

Pedestal Model	Pedestal Width	Mixed Bohm/gyro-Bohm model		Multi-mode model	
		P_α (MW)	Fusion Q	P_α (MW)	Fusion Q
1	$\Delta\alpha\rho s^2$	13.9	1.7	49.4	6.2
2	$\Delta\alpha(\rho Rq)^{1/2}$	11.7	1.5	47.3	5.9
3	$\Delta\alpha R(\beta_{0,ped})^{1/2}$	16.3	2.0	51.2	6.4

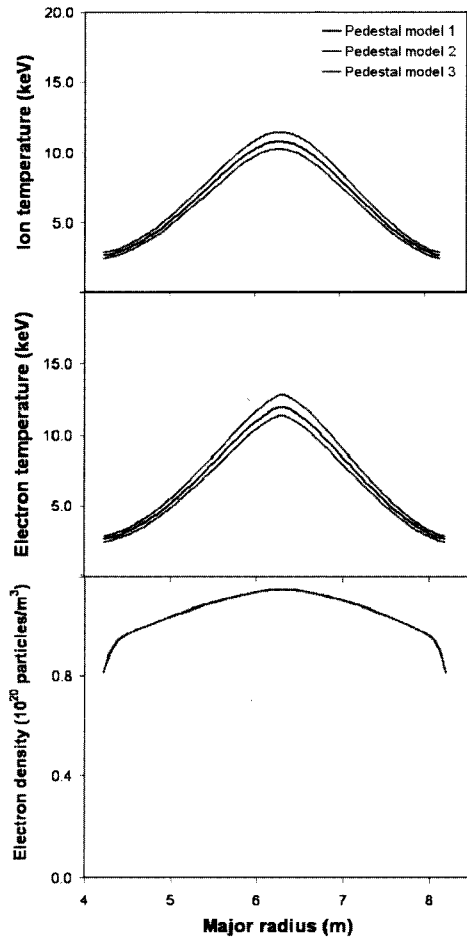


Fig. 1: Profiles for ion temperature (top), electron temperature (middle) and electron density (bottom) are shown as a function of major radius at a time of 300 sec. These BALDUR simulations are carried out using Mixed B/gB core transport model and using three different pedestal temperature models.

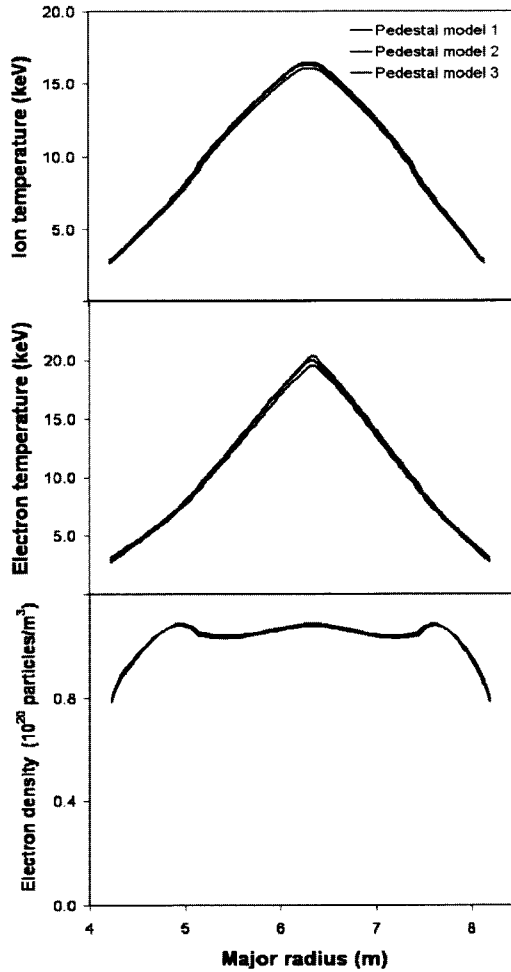


Fig. 2: Profiles for ion temperature (top), electron temperature (middle) and electron density (bottom) are shown as a function of major radius at a time of 300 sec. These BALDUR simulations are carried out using MMM95 core transport model and using three different pedestal temperature models.

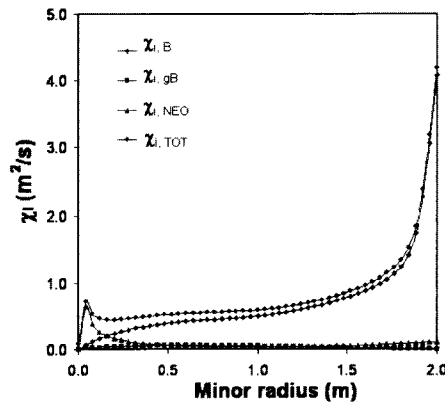


Fig. 3: Ion diffusivities from the Mixed B/gB transport model are shown as a function of minor radius at a time of 300 sec. This simulation is carried out using the pedestal temperature model based on magnetic and flow shear stabilization width model (pedestal model 1).

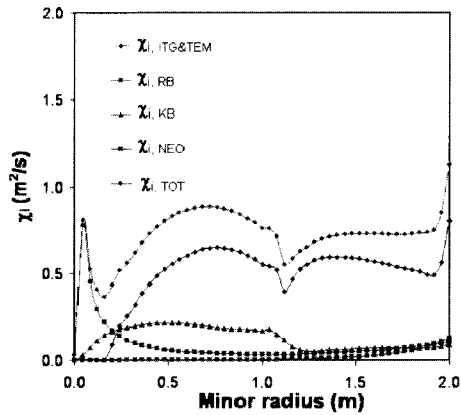


Fig. 4: Ion diffusivities from the MMM95 transport model are shown as a function of minor radius at a time of 300 sec. This simulation is carried out using the pedestal temperature model based on magnetic and flow shear stabilization width model (pedestal model 1).

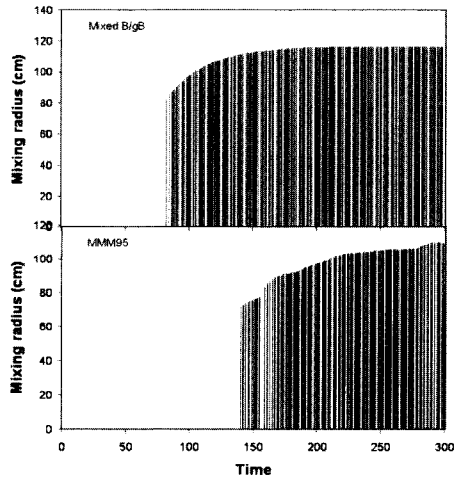


Fig. 5: Sawtooth mixing radius is plotted as a function of time. This simulation is carried out using the pedestal temperature model based on the magnetic and flow shear stabilization width model (pedestal model 1). The top panel is the simulation using Mixed B/gB and the bottom panel is the simulation using MMM95.

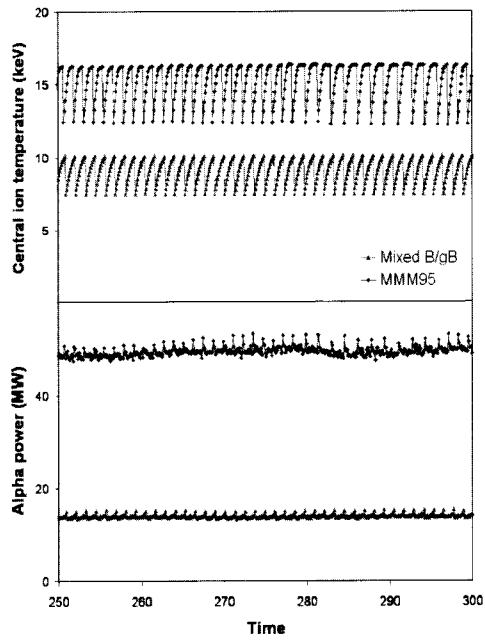


Fig. 6: Central ion temperature (top panel) and alpha power (bottom panel) are plotted as a function of time. This simulation is carried out using the pedestal temperature model based on the magnetic and flow shear stabilization width model (pedestal model 1).